N O T I C E

THIS DOCUMENT HAS BEEN REPRODUCED FROM MICROFICHE. ALTHOUGH IT IS RECOGNIZED THAT CERTAIN PORTIONS ARE ILLEGIBLE, IT IS BEING RELEASED IN THE INTEREST OF MAKING AVAILABLE AS MUCH INFORMATION AS POSSIBLE

NASA

Technical Memorandum 82086

MAGNETIC LOOP BEHIND AN INTERPLANETARY SHOCK: VOYAGER, HELIOS AND IMP-8 OBSERVATIONS

L. Burlaga, E. Sittler,
F. Mariani and R. Schwenn

FEBRUARY 1981

MAGNETIC LOOP BEHIND AN INTERPLANETARY SHOCK:
VOYAGER, HELIOS AND IMP-8 OBSERVATIONS

by

L. Burlaga

E. Sittler

NASA/Goddard Space Flight Center

Laboratory for Extraterrestrial Physics

Greenbelt, MD   20771

F. Mariani

Istituto di Fisica Universita

Piazzale delle Scienze

Rome, Italy

R. Schwenn

Max-Planck-Institut fur Aeronomie

Postfach 20

3411 Katlenburg-Lindau 3

FEDERAL REPUBLIC OF GERMANY

ABSTRACT

Magnetic field and plasma data from 5 spacecraft (Voyager 1 and 2, Helios 1 and 2, and IMP-8) were used to analyze the flow behind an interplanetary shock. The shock was followed by a turbulent sheath in which there were large fluctuations in both the strengtn and direction of the magnetic field. This in turn was followed by a region (magnetic cloud) in which the magnetic field vectors were observed to change by rotating nearly parallel to a plane, consistent with the passage of a magnetic loop. This loop extended at least 30° in longitude between 1-2 AU, and its radial dimension was approximately 0.5 AU. In the cloud the field strength was high and the density and temperature were relatively low. Thus the dominant pressure in the cloud was that of the magnetic field. The total pressure inside the cloud was higher than outside, implying that the cloud was expanding as it moved outward, even at the distance of 2 AU. The momentum flux of the cloud at 2 AU was not higher than that of the preshock plasma, indicating that the cloud was not driving the shock at this distance. It is possible, however, that the shock was driven by the cloud closer to the sun where the cloud may have moved faster. An extraordinary filament was observed at the rear of the cloud. It was bounded by current sheets whose orientations were preserved over at least 0.12 AU and which were related to the plane of maximum variance of the magnetic field in the cloud.

1. Introduction

The existence of unusual magnetized clouds of plasma emitted by the active sun was proposed by Morrison (1954) as a cause of world-wide decreases in cosmic ray intensity, lasting for days and correlated roughly with geomagnetic storms. Cocconi et al. (1958) suggested that the magnetic field lines in such a cloud form an extended loop, the field lines being anchored in the sun, and they called such a loop an "elongated tongue" and a "magnetic bottle". A similar concept was discussed more quantitatively by Piddington (1958), who considered the additional possibility that a loop could become detatched from the sun by magnet's field reconnection, forming closed magnetic field lines in the solar wind (a magnetic "bubble"). Gold (1959) proposed that the magnetic loop might be preceded by a shock wave (see also Gold, 1955, 1962). All of these authors envisaged that the magnetic cloud or loop is formed by motion of plasma ejected from a flare or some other transient solar disturbance. None was very specific about the 3-dimensional configurations of the magnetic field

Magnetic fields in transient flows behind shocks (hereafter called magnetic clouds) have been recorded by many spacecraft and discussed in many publications. However, the geometry of the lines of force is difficult to determine from measurements at a single spacecraft, and direct evidence for magnetic field line configurations in the form of loops or bubbles has been elusive (see Hundhausen, 1972). Montgomery et al. (1974) and Gosling et al. (1973) suggested that low temperatures which they observed behind shocks were associated with magnetic bubbles, but they presented no magnetic field observations. Similarly, Palmer et al. (1978) and Bame et al. (1980) speculated that bi-directional anisotropies which they observed behind some shocks were associated with magnetic bubbles, but again no magnetic field observations were presented. Statistical evidence for magnetic loops behind shocks was presented by Pudovkin et al. (1977, 1979) based on the magnetic field data compiled by King (1977); however, they did not consider th plasma observations. Bobrov (1979) noted that in some flare-associated streams one component of $\underset{\wedge}{B}$, viz. that parallel to the earth's geomagnetic equator, varies systematically in a way that he suggested is consistent with a closed magnetic loop in that plane.

Schatten et al. (1968) presented evidence for a magnetic loop in the
equatorial plane using magnetic field data from IMP-3. Observations of
monotonic, 2-dimensional variations in the magnetic field behind a shock,
consistent with the passage of a magnetic loop or tightly wound helix, were
discussed by Burlaga and Klein (1980).

This paper investigates the configuration of the magnetic field in a
flow behind a shock observed at 2 AU on January 6, 1978 and at ∿ 1 AU on
Jaunary 3. It will be shown that the magnetic field in the "driver" gas
closely resembles that of an extended loop with ordered fields as proposed
by Cocconi et al. (1958) and Piddington (1958). However, there is a
region (a sheath) between the shock and the stream in which the field is
strong and turbulent. We discuss data from 5 spacecraft--Voyagers 1 and 2,
Helios 1 and 2, and IMP-8.

The positions of the spacecraft are very favorable for this
investigation, as shown in Figure 1. Voyagers 1 and 2 w re close to one
another at 2 AU; Helios 1 was near the Voyager-sun line, at 0.9 AU; and
Helios 2 and IMP-8 were close to one another near 1 AU. Voyagers 1 and 2
were 30°E of the earth. This distribution of spacecraft makes it possible
to put a significant lower limit on the azimuthal extent of the cloud.

The data which are discussed below are from the magnetic field and
plasma experiments listed in Table 1, which also identifies the Principal
Investigator (PI) for each experiment. The IMP-8 magnetic field and plasma
data discussed below are from a tape compiled by King (1979) from data
deposited by the Principal Investigators in the National Space Science Data
Center of NASA/Goddard Space Flight Center. The Voyager magnetic field and
plasma experiments are described in the papers of Behannon et al. (1977)
and Bridge et al. (1977), respectively. The Helios magnetic field
experiment (Rome/GSFC) and plasma experiment are described in Scearce et
al. (1975) and Schwenn et al. (1975) respectively.

2. Overview of the January 1978 Event

The basic characteristics of the magnetic field and flow behind the shock are illustrated by the Voyager 1 magnetic field and plasma data shown in Figure 2. The nearly monotonic variation of the latitude of B (δ, in heliographic coordinates) from large southern directions to large northern directions and the higher than average magnetic field strengths (F) is consistent with the passage of a magnetic loop (see Section 3). It is useful to speak of the magnetic field in the post-shock ejecta without reference to a specific configuration, and for this purpose the term "magnetic cloud" is convenient. The magnetic cloud passed the spacecraft between approximately mid-day on January 6 and mid-day on January 8, 1978, as indicated by the vertical dashed lines in Figure 2. There is an uncertainty of a few hours in the times of the boundaries. Our choice for the time of the front (early) boundary is based on the sudden increase in field strength and the change to large southern directions. Note that the proton temperature (T_p) dropped abruptly by an order of magnitude across this boundary, and the proton density (n) fell appreciably shortly afterward. Our choice for the time of the rear (later) boundary is based primarily on the sudden decrease in δ from an extreme northern direction. One might argue that this boundary occurred later or that the boundary is diffuse and filamentary; this ambiguity is not important for the objectives of this paper. Note that the density increased abruptly by an order of magnitude at the rear boundary, but the magnetic field strength, temperature and bulk speed did not return to near-average solar wind values across this boundary.

Inside the magnetic cloud the field strength was high and the direction varied smoothly. The density, the proton temperature (T_p) (moment temperature) and the electron temperature (T_e) (core temperature) were relatively low and irregular and the speed was high with a familiar stream profile. Such a pattern in the plasma parameters has previously been shown to be characteristic of transient post-shock flows (see, e.g., Hundhausen, 1972; Montgomery et al., 1974; Gosling et al. 1973; Dryer, 1975; Burlaga et al., 1980; and Burlaga and King (1979). In any case, the profiles do not resemble those in stationary flows.

Ahead of the magnetic cloud there was a region in which the magnetic field was extremely turbulent as indicated by the large fluctuations in both the magnetic field strength and direction (see Figure 2). The plasma in this region was unusually hot and dense. The transition from ambient conditions to this region occurred during a data gap lasting 6.5 hours. Across this gap, F, n, V, T_p and T_e all increased, suggesting the presence of a shock wave. Voyager 2, which was located close to Voyager 1, did observe a shock, and we calculated that this shock should have passed Voyager 1 at the time indicated by the arrow in the top panel of Figure 2, i.e., in the data gap. Thus it is fairly certain that the turbulent, hot, dense plasma preceding the magnetic cloud in Figure 2 was produced by a shock wave. We infer that 1) somewhere between the sun and 2 AU the shock was driven by the plasma carrying the magnetic cloud and 2) this cloud was preceded by a turbulent sheath consisting of shocked plasma from the upstream region, analogous to the earth's magnetosheath. Further evidence in support of these inferences is given below.

The Helios 2 observations of the January 1978 event are shown in Figure 3. A magnetic cloud is identified by the high field strengths and the characteristic variation in the latitude of the magnetic field direction (here the latitude is given in solar ecliptic coordinates and it is denoted by θ to distinguish it from the heliographic latitude angle λ used in the Voyager data reduction system). Our estimated positions of the front and rear boundaries of the magnetic loop are shown by the vertical dashed lines in Figure 3. The front boundary position was chosen on the basis of the sudden increase in F, and the rear boundary position was chosen on the basis of the drop in θ toward the nominal spiral-field value. Again the boundaries are not determined unambiguously, and one might argue that they are not thin or that they should be chosen a few hours earlier or later, but this is not important for our principal objectives.

Helios 2 observed that the density and temperature were relatively low in the magnetic cloud and the speed was higher than the ambient value, just as in the Voyager 1 data. In this case, however, the stream was followed by a smaller stream, which is possibly one reason for the ambiguity in the

rear boundary of the magnetic cloud. We regard this small stream as a separate flow system, and it will not be considered further.

The magnetic cloud and transient flow at Helios 2 were preceded by a hot region in which the magnetic field strength was high and both the strength and direction were highly variable. The fluctuations in the magnetic field direction are described in Figure 3 by the variance, σ^2, of the Cartesian components of $\underline{B}$. We interpret this hot turbulent region as a sheath consisting of shocked plasma, as discussed above in reference to the Voyager 1 data. A shock was observed by Helios 2 at 1450 UT on Jaunary 3, 1978. Its local speed was 480 km/s and its normal was $\phi_n \sim 37^{\circ}$, $\theta_n \sim 4^{\circ}$. The source of the flow system could be one of three flares observed on Jaunary 1st: 1) a 2N flare at 0554 UT at S20° E34° in McMath region 15083, 2) a 1N flare at 0727 UT at S17°, E 10° in McMath region 15081, 3) a 2N flare at 2145 UT at S21°, E06° in McMath region 15081. We cannot make a unique association of the flow with any one of these events. In summary, the Helios 2 data, like the Voyager 1 data, show three phenomena: a magnetic cloud in a fast stream, a shock which is presumably driven by the stream somewhere between the sun and $\sim$ 1 AU, and a sheath between the shock and the magnetic cloud.

3. Size of the Magnetic Cloud

The magnetic field strength profiles and the magnetic field latitude angle profiles for Voyagers 1 and 2, IMP-8 and Helios 2 are compared in Figure 4. (There are no Helios 1 magnetic field data from the Rome/GSFC experiment for this event.) The time scales for each spacecraft have been shifted such that the shock falls on the solid vertical line in Figure 4, i.e., in effect we set t = 0 at the time of the shock (see Table 2). The calculated shock time was used for Voyager 1, as described above in the discussion of Figure 2. The front boundary of the magnetic cloud observed by Helios 2 occurred $\sim$ 16 hours after the shock. We assume that this separation is approximately the same at all spacecraft and we represent the front boundary by a single dashed vertical line in Figure 4. This boundary was not seen at Voyager 2 due to a data gap. The front boundary at IMP may have occurred a few hours earlier than implied by the dashed line in Figure

4, but that is unimportant for our purpose. The rear boundary observed by Helios 2 was much closer to the shock than that observed by Voyager 1 or Voyager 2. IMP, which was close to Helios 2, observed a similar result.

The size of the magnetic cloud can be estimated using the times of the boundaries shown in Figure 4 and the spacecraft positions at those times. It is convenient to do this by plotting the positions of all the boundaries at one instant, which we take to be hour 22 on January 6. These positions were calculated using the measured bulk speeds at each boundary and assuming that the plasma moved radially away from the sun at a constant speed between $\sim$ 1 AU and $\sim$ 2 AU. The positions thus obtained are shown by the dots in Figure 5. An uncertainty of $\sim$ ± 8 hrs in the times of the boundaries corresponds to an uncertainty of $\sim$ 0.08 AU in their positions, as indicated by the error bar shown at the dot on the IMP-sun line. Thus the error bars are small compared to the dimensions of the magnetic cloud. The dots in Figure 5 have been connected by eye to delineate the general shape of the cloud. One can draw two significant conclusions about the size of the magnetic cloud from Figure 5: 1) Its azimuthal extent between 1 and 2 AU was at least 30°, and 2) its radial dimension was approximately 0.5 AU.

4. Magnetic Field Configuration in the Cloud

The familiar two-dimensional sketches of a magnetic loop suggest but never show that the magnetic field is planar, i.e., that the lines of force are plane curves and there is one dimension in which the magnetic field does not change. The minimum variance analysis of Sonnerup and Cahill (1967) has frequently been used to identify and describe planar magnetic field configurations associated with thin current sheets in the solar wind and planetary magnetospheres. We have used this method to analyze the magnetic field configurations in the magnetic cloud described above (see also Burlaga and Klein, 1980, and Klein and Burlaga, 1981). The only modification required is the use of hour averages rather than high resolution measurements, corresponding to the larger scale of the magnetic clouds. We carried out a minimum variance analysis for each of the data sets--Voyager 1, Voyager 2, Helios 2 and IMP-8. Since the front and rear

boundaries of the magnetic cloud are ambiguous, we did the minimum variance analysis for several intervals. The results are not sensitive to the boundary times within the uncertainties discussed in Section 2 so we present only the results corresponding to the boundaries shown in Figure 4.

Figure 6 shows the results obtained from the Voyager 1 and 2 magnetic cloud data. The Z-direction is the direction in which the variance of $\hat{B}$ is a minimum, and the X-Y plane is normal to $\hat{z}$. In both cases, $\hat{B}$ rotates relatively smoothly through a large arc in the X-Y plane. The components of $\hat{B}$ normal to this plane are very small, and they are consistent with zero within the uncertainties of the method (see Lepping and Behannon, 1980; Siscoe and Suey, 1972). The normal to the plane of maximum variance may be specified by its heliographic longitude, λ_n, and latitude, δ_n. For Voyager 2 and Voyager 1, respectively, $\lambda_n = 234°$ and $231°$ while $\delta_n = -17°$ and $-42°$. Thus, the Voyager 1 and 2 results are consistent with one another within $\hat{\nu}$ $\pm 13°$, which is approximately the error expected from the minimum variance analysis, and the average normal at their positions is $\lambda_n = 232°$ and $\lambda_n = -26°$.

The minimum variance analysis results obtained using the magnetic cloud fields measured by IMP-8 and Helios-2 are shown in Figure 7. Again it .s found that the magnetic field rotates relatively smoothly through a large arc, and the components of $\hat{B}(t)$ normal to this plane are small and consistent with zero. For IMP-8 and Helios-2, respectively, the normals are given by $\lambda_n = 230°$, $203°$ and $\delta_n = -24°$, $-46°$ in solar heliographic coordinates. Thus the IMP-8 and Helios-2 results are consistent with one another within $\hat{\nu}$ $\pm 15°$ and the average normal at their positions is $\lambda_n = 218°$, $\delta_n = -34°$.

Comparing the normals obtained from the minimum variance analysis using data from Voyagers 1 and 2 with those obtained using data from Helios-2 and IMP-8, (which were $\sim$ 1 AU closer to the sun than Voyager 1 and 2 and $\sim$ 30° E of the Voyager-sun line) we find nearly the same results for both positions. In particular, the average of the normals measured by Voyagers ($\lambda_n = 232°$, $\delta_n = -26°$) agrees with the average of the IMP-8/Helios-2 normals ($\lambda_n = 218°$, $\delta_n = -34°$) within the accuracy with which the normals

can be determined. These results demonstrate that the magnetic field
configuration is substantially planar and highly organized on a
large-scale.

A qualitative sketch of a possible magnetic field configuration in the
cloud is shown in Figure 8. This configuration is consistent with the
observations, but it is not uniquely determined. It is based on the
magnetic field observations in Figure 2-4, the cloud structure shown in
Figure 5, and the results of the minimum variance analysis described above.
Figure 8 shows the magnetic cloud as a circular cylinder whose axis lies in
the equatorial plane, making an angle of nearly 90° with respect to the
radial direction in accordance with Figure 5. Since we have no information
out of the ecliptic, the cross section could also be drawn as an ellipse or
an irregular form and the axis might be inclined with respect to the
ecliptic. The magnetic field lines in the cloud lie in a plane which is
inclined 35° with respect to the ecliptic. They are drawn in Figure 8 as
closed circular loops, but they could be more complicated closed curves or
they might be open "tongues" as described by Cocconi et al. (1958).
Measurements out of the ecliptic are needed to distinguish among these
alternatives. There is a further ambiguity owing to the uncertainty in
determining the component of $\underset{\sim}{B}$ normal to the plane of maximum variance,
i.e., it is possible that the lines of force form very tightly wound
helices. Finally, there is some evidence that the axis of the circular
cylinder is slightly bent. Thus, Figure 8 is schematic and non-unique, but
it is consistent with the observations and represents some basic
characteristics of the magnetic cloud.

5. Plasma Parameters in the Magnetic Cloud

In order to compare the bulk flow measurements made by Voyagers 1 and
2, Helios 1 and 2 and IMP-8, it is convenient to discuss each of the flow
parameters separately. Figure 9 shows the density profiles measured by
each of the spacecraft. The time scales have been shifted such that the
shocks are on the same vertical line (see Table 2). The vertical dashed
lines in Figure 9 represent the magnetic cloud boundaries chosen as
described in Section 2 in reference to Figure 4. (The rear boundary of the

magnetic cloud seen by Helios 1 could not be identified with certainty.)
Inside the magnetic cloud the density is highly variable, often changing by
nearly an order of magnitude in a few hours. Generally the density inside
the magnetic cloud is significantly lower than average, but there are
occasional fluctuations which reach the ambient value. Such low densities
have often been observed in flare ejecta. There are two possible
explanations for them, not mutually exclusive: 1) The density in the
magnetic cloud was relatively low at the sun where it was ejected, and/or
2) the magnetic cloud expanded as it moved from the sun to the spacecraft
at $R > 2$ AU. Evidence for expansion of the magnetic cloud will be
discussed in the next section.

The speed profiles measured by the 5 spacecraft are shown in Figure 10.
All of the spacecraft observed fast (> 400 km/s) plasma in the magnetic
cloud, but the individual speed profiles differ appreciably. Voyager 1
observed a familiar stream profile, with a rapid rise to a maximum speed of
nearly 700 km/s followed by a monotonic decline to lower speeds. Voyager
2, on the other hand, observed a flatter speed profile, with speeds between
500 km/s and ~ 600 km/s; however, it should be noted that higher speeds
might have occurred in the large data gap on January 7. The IMP and Helios
2 speed profiles are similar to one another, both showing a decrease from ~
650 km/s to ~ 450 km/s in the magnetic cloud. It appears that material in
the rear of the magnetic cloud near the positions of IMP and Helios-2 was
accelerated by a stream which was overtaking the cloud. Material ahead of
the cloud was also moving very fast, perhaps because the magnetic cloud was
embedded in a larger stream or perhaps because the cloud accelerated
material ahead of it. The Helios-1 speed profile is the most complicated.
The shock and magnetic cloud were advancing into a fast (~ 600 km/s)
plasma, so the post-shock speeds were much higher than in the other cases.
This is possibly a latitude effect (see Figure 1), although it was not seen
by Voyagers 1 and 2. There was no well-defined rear boundary, and there
was no large change in the speed profile at the front boundary. However,
the speeds inside the cloud seen by Helios 2 were at least as high as those
observed by the other spacecraft. We conclude that material inside the
magnetic cloud as a whole was moving significantly faster than the average
solar wind speed, but no single, characteristic speed profile was observed
by all of the spacecraft.

Finally, consider the temperature profiles, shown in Figure 11. All of the spacecraft observed lower than average temperatures near the cen,er of the magnetic cloud and near-average temperatures close to its boundaries. Large fluctuations in the temperature were observed, and one cannot draw a smooth representative temperature profile. In the sheath, the temperatures were higher than average, presumably owing to heating by the shock. The Helios-1 profile is anomalous in that the temperature drops abruptly a few hours after the shock, suggesting that the shock had moved through some relatively cool plasma at that position.

6. Dynamics of the Magnetic Cloud

In this section we examine the Voyager 1 and 2 momentum flux and pressure profiles in search of information about the dynamical properties of the magnetic cloud. The momentum flux, ρV^2, the total pressure $(P_T = nk (T_e + T_p) + B^2/8\pi)$ and the ratio of the thermal pressure to the magnetic pressure, $\beta_T = nk (T_e + T_p)/(B^2/8\pi)$ are shown in Figures 12 and 13 for Voyager 1 and Voyager 2, respectively.

The overall momentum flux profile observed by Voyager 1 resembles that observed by Voyager 2, but there are significant differences in detail owing to the large fluctuations in n and T. The most significant result is that for the most part the momentum flux inside the magnetic cloud is not appreciably higher than that ahead of the shock. This suggests that at the positions of V1 and V2 ($\sim$ 2AU) the shock was no longer being strongly driven by the magnetic cloud, even though the cloud was moving supersonically with respect to the ambient solar wind. One possible scenario is that near the sun both the density and speed were high in the cloud giving a momentum flux large enough to produce a shock there. In transit to 2 AU the magnetic cloud expanded causing a reduction in the density such that the momentum flux inside the cloud was not large when it arrived at V1 and V2. The shock continued to propagate outward even though it was not driven by the cloud at 2 AU.

The pressure profiles in Figures 12 and 13 show that even at ⁓ 2 AU the total pressure inside the magnetic cloud was somewhat higher than the ambient pressure ahead of the shock. This implies expansion of the cloud at 2 AU as a result of the high pressure, and it suggests that there was expansion close to the sun. The expansion was caused primarily by the magnetic pressure rather than the thermal pressure, for $\beta_T \lesssim 1$ inside the magnetic cloud. Note that in some parts the magnetic cloud the thermal pressure was negligible--$\beta < 0.05$. In general, the magnetic field energy was dominant in the magnetic cloud, which may explain why rather large fluctuations in density and temperature could persist inside the magnetic cloud. The high magnetic energy density is consistent with the observations of smoothly varying magnetic fields inside the cloud and the ordered large-scale configuration of the cloud discussed in Section 4.

7. Discontinuities in the Flow Observed by V1 and V2

A remarkable filament in the V2 magnetic field and plasma data is shown in Figure 14 near noon on January 8. It is seen most clearly as an enhancement in density and a depression in field strength, but one can also see a depression in the temperature. Thus, the filament is a dense, cool region with relatively low magnetic field strengths. The boundaries of the filament are very thin when viewed on this scale. The filament is shown at higher resolution (1.92 sec averages) in Figure 15a. Even at this resolution the boundaries of the V2 filament appear as step functions in F and n, and abrupt changes are also seen in T and V. The front boundary of the filament (A) is associated with a current sheet (directional discontinuity) as evidenced by the large, rapid, step-like change in δ and λ. The rear boundary (B) is also associated with a current sheet, but this is not as clearly defined as A.

The filament was also seen by V1, which was 0.12 AU from V2. This may be seen by comparing Figures 14 and 2, and by comparing the results in Figure 15a and b. The filament is not as well defined in the V1 data as it is in the V2 data. In particular, it is difficult to identify a rear boundary at V1 corresponding to B at V2 (see Figure 15). However, the front boundary (A and A') is clearly seen by both spacecraft with

essentially the same qualitative signature in F, θ, λ, n, T_p and T_e. (V1 quantitative estimates not yet available in such special regions where electron core temperatures are $\lesssim 3 \times 10^{4}$°K during the cruise 1 phase of the mission.)

The nature of the boundaries of the filament can be determined by considering the variation of the total pressure $P_T = nk (T_p + T_e) + F^2/(8\pi)$ across the filament. This is shown for V2 in Figure 16, where it is seen that there is essentially no change in P_T across the filament and its boundaries. According to the theory of MHD discontinuities (see Landau and Lifshitz, 1960 and Burlaga, 1971) this excludes the possibility that the discontinuities are fast or slow shocks. Shocks are also excluded by the signs of the changes in n, T and B. The constancy of P_T indicates that the discontinuities are tangential discontinuities (TD), rotational discontinuities (RD) or contact discontinuities (CD). A CD is ruled out by the change in magnetic field direction, and an RD is effectively ruled out by the very large changes in F and n. Thus, the boundaries of the filament must be tangential discontinuities.

It is possible to determine the orientations of the surfaces bounding the filament by examining the internal structure of the current sheets (Sonnerup and Cahill, 1967; Siscoe et al., 1968; Burlaga et al., 1977). The Sonnerup-Cahill method gives further evidence that the boundaries are TDs, since the component of $\underset{\sim}{B}$ normal to the plane of maximum variance is less than 15% of the mean field. Using the method of Siscoe et al. (1968), which is more accurate for TDs than the Sonnerup-Cahill method, we obtain the normals of the surfaces A, A' and B listed in Table 3. The normal of the plane of maximum variance of $\underset{\sim}{B}$ in the magnetic cloud (see Section 3), is also given in Table 3. These results are shown graphically in Figure 17, where the intersections of the surfaces with the ecliptic plane and a meridian plane are shown by solid line segments, and the corresponding intersections of the maximum variance plane of $\underset{\sim}{B}$ are shown by dashed line segments. Table 3 and Figure 17 reveal three significant results. First, the orientation of surface A at V2 is similar to that of surface B at V2, as one might expect for a filament. Second, the orientation of A at V2 is very similar to that of A' at V1, despite the relatively large separation

(0.12 AU) between the two spacecraft. (Previous studies by Burlaga and Ness, 1969 and Denskat and Burlaga, 1977, showed that the orientation of a current sheet may change appreciably on a scale of 0.005 AU.) Third, the normals of the small-scale filament boundaries lie close to the normal to the maximum variance plane of the magnetic field vectors in the mesoscale magnetic cloud (see Figures 6 and 7). In other words the orientations of the small scale current sheets bounding the filament are related to the mesoscale configuration of the magnetic field in the stream behind the shock. It will be of interest to examine other clouds in order to determine the generality of this conclusion, but that is outside the scope of this paper.

Figure 17 shows the orientations of four other discontinuities: the shock at V2, two directional discontinuities in the sheath seen by V1 (D and E), and a directional discontinuitity observed by V1 near or in the front boundary of the magnetic cloud. These four surfaces are nearly parallel to one another, but their orientations differ from those of the filament boundaries and the maximum variance plane of the magnetic cloud. This difference is consistent with presence of two types of flow regimes--the flow associated with the magnetic cloud and the flow in the sheath. The orientations of the current sheets ahead of the magnetic cloud may be related to the geometry of the surface of the cloud. In particular they are consistent with the boundary being an element of a nearly spherical front as shown in Figure 5.

8. Summary

We have analyzed a flow system consisting of a shock, a turbulent sheath, and an ordered "magnetic cloud" in transient ejecta associated with the shock, using magnetic field and plasma data from 5 spacecraft. The emphasis is on the magnetic cloud which was identified by a characteristic variation of the latitude angle of the magnetic field. The size of the cloud was found to be $\hat{\sim}$ 0.5 AU in radial extent and $>$ 30° in azimuthal extent, and the front boundary was nearly normal to the radial direction. As the magnetic cloud moved past each of the spacecraft the magnetic field direction was observed to change by rotating nearly parallel

to a plane. Thus, the magnetic field configuration in the cloud was
essentially two dimensional. The orientation of this plane of maximum
variance with respect to the spacecraft-sun line and solar equatorial plane
was the same at all of the spacecraft within $\sim$ 20°. These results suggest
that the lines of force in the magnetic cloud formed loops, but it could
not be determined whether these loops were open or closed.

Inside the magnetic cloud the speed was high and the density and
temperature were relatively low, especially near the middle of the cloud.
The total pressure in the cloud was higher than the ambient pressure at
2 AU, indicating that the cloud was probably expanding at 2 AU and, by
inference, within 2 AU as well. The magnetic pressure was larger than the
thermal (ion plus electron) pressure, indicating that the expansion was
driven primarily by the magnetic field which presumably originated in some
transient process at the sun. Expansion driven by the high magnetic field
pressure inside the cloud is at least one cause of the low density and
temperatures in the magnetic cloud; the input conditions might be another
cause.

The momentum flux in the cloud at 2 AU was not generally higher than
that ahead of the cloud, yet the cloud was preceded by a shock. It is
suggested that the shock might have driven by the stream carrying the
magnetic cloud when it was near the sun, but that the momentum flux
decreased in transit to 1 AU owing to expansion and perhaps deceleration so
that at 2 AU the shock was no longer driven, but rather moved on ahead of
the cloud by virtue of the motion it acquired earlier. Of course, we
cannot exclude the possibility that the shock and ejecta were created
independently at the sun.

At the rear of the magnetic cloud there was a most unusual filament
characterized by high n and low B and T, with very thin boundaries having
the nature of tangential discontinuities. This filament was in equilibrium
with the medium in which it was embedded. Its boundaries (current sheets)
were nearly parallel to the plane of maximum variance of $\underset{\sim}{B}$ in the magnetic
cloud. Current sheets in the sheath ahead of the magnetic cloud had
different orientations, more nearly perpendicular to the radial direction
and parallel to the surface of the shock wave.

ACKNOWLEDGMENTS

REFERENCES

Bame, S. J., J. R. Asbridge, W. C. Feldman, J. T. Gosling, and R. D.
Zwickl, Bi-directional streaming of solar wind electrons > 80 eV: ISEE
evidence for a closed-field structure within the driver gas of an
interplanetary shock, Geophys. Res. Lett., in press, 1980.

Behannon, K. W., M. H. Acuna, L. F. Burlaga, R. P. Lepping, N. F. Ness, and
F. M. Neubauer, Magnetic field experiment for Voyagers 1 and 2, Space
Sci. Rev., 21, 235, 1977.

Bobrov, M. S., Magnetic classification of solar wind streams, Planetary
Space Sci., 27, 1461, 1979.

Bridge, H. S., J. W. Belcher, R. J. Butler, A. J. Lazarus, A. M. Mavretic,
J. D. Sullivan, G. L. Siscoe, and V. M. Vasyliunas, The plasma
experiment on the 1977 Voyager mission, Space Sci. Rev., 21, 259, 1977.

Burlaga, L. F. and N. F. Ness, Tangential discontinuities in the solar
wind, Solar Phys., 9, 467, 1969.

Burlaga. L. F., Hydromagnetic waves and discontinuities in the solar wind,
Space Sci. Rev., 12, 600, 1971.

Burlaga, L. F., J. F. Lemaire, and J. M. Turner, Interplanetary current
sheets at 1 AU, J. Geophys. Res., 82, 3191, 1977.

Burlaga, L. F. and J. H. King, Intense interplanetary magnetic fields
observed by geocentric spacecraft during 1963-1975, J. Geophys. Res.,
84, 6633, 1979.

Burlaga, L. F. and L. Klein, Magnetic clouds in the solar wind, NASA TM
80668, 1980.

Burlaga, L., R. Lepping, R. Weber, T. Armstrong, C. Goodrich, J. Sullivan,
D. Gurnett, P. Kellogg, E. Keppler, F. Mariani, F. Neubauer, and R.
Schwenn, Interplanetary particles and fields, Nov. 22 - Dec. 6, 1977:
Helios, Voyager and IMP observations between 0.6 AU and 1.5 AU, J.
Geophys. Res., 85, 2227, 1980.

Cocconi, G., T. Gold, K. Greisen, S. Hayakawa, and P. Morrison, The cosmic
ray flare effect, Nuovo Cimento, 8, 161, 1958.

Denskat, K. U. and L. F. Burlaga, Multispacecraft observations in
microscale fluctuations in the solar wind, J. Geophys. Res., 82, 2693,
1977.

Dryer, M., Interplanetary shock waves: Recent developments, Space Sci.
Rev., 17, 277, 1975.

Gold, T., Contribution to discussion, in gas dynamics of cosmic clouds, p. 103, North-Holland Publishing Company, Amsterdam, 1955.

Gold, T., Plasma and magnetic fields in the solar system, J. Geophys. Res., 64, 1665, 1959.

Gold, T., Magnetic storms, Space Sci. Rev., 1, 100, 1962.

Gosling, J. T., V. Pizzo, and S. J. Bame, Anomalously low proton temperatures in the solar wind following interplanetary shock waves: Evidence for magnetic bottles?, J. Geophys. Res., 78, 2001, 1973.

Hundhausen, A. J., Coronal Expansion and Solar Wind, Springer-Verlag, New York, 1972.

King, J. H., Interplanetary Medium Data Book, NSSPC/WDC-A-RAS, 77-04, 1977.

King, J. H., Interplanetary Medium Data Book, Supplement 1, NSSPC/WDC-A-RAS, 79-04, 1979.

Klein, L. and L. Burlaga, A statistical study of interplanetary magnetic clouds at 1 AU, J. Geophys. Res., to be submitted, 1981.

Landau, L. D. and E. M. Lifshitz, Electrodynamics of continuous media, p. 224, Addison-Wesley, Reading, Massachusetts, 1960.

Lepping, R. P. and K. W. Behannon, Magnetic field directional discontinuities: 1 Minimum variance errors, to appear in J. Geophys. Res., 1980.

Montgomery, M. D., J. R. Asbridge, S. J. Bame, and W. C. Feldman, Positive evidence for closed magnetic structures in the solar wind associated with interplanetary shock waves, J. Geophys. Res.,

Morrison, P., Solar-connected variations of the cosmic rays, Phys. Rev., 95, 646, 1954.

Palmer, I. D., F. R. Allum, and S. Singer, Bidirectional anisotropies in solar cosmic ray events: Evidence for magnetic bottles, J. Geophys. Res., 83, 75, 1978.

Piddington, J. H., Interplanetary magnetic field and its control of cosmic-ray variations, Phys. Rev., 112, 589, 1958.

Pudovkin, M. I., S. A. Zaitseva, and E. E. Benevolenska, The structure and parameters of flare streams, J. Geophys. Res., 84, 6649, 1979.

Pudovkin, M. I., S. A. Zaitseva, L. P. Oleferenko, and A. D. Chertkov, The structure of the solar flare stream magnetic field, Solar Phys., 54, 155, 1977.

Scearce, C., S. Cantarano, N. Ness, F. Mariani, and R. Terenzi, The
Rome-GSFC magnetic field experiment for Helios A/B (E3),
Raumfahrtforschung, 19, 237, 1975.

Schatten, K. H., N. F. Ness, and J. M. Wilcox, Influence of a solar active
region on the interplanetary magnetic field, Solar Phys., 5, 240, 1968.

Schwenn, R. H. Rosenbauer, and H. Miggenrieder, Das plasma experiment auf
Helios (E1), Raumfahrtforschung, 19, 226, 1975.

Siscoe, G. L., and R. W. Suey, Significance criteria for variance matrix
applications, J. Geophys. Res., 77, 1321, 1972.

Siscoe, G., L. Davis, Jr., P. J. Coleman, Jr., E. J. Smith, and D E. Jones,
Power spectra and discontinuities of the interplanetary magnetic field:
Mariner 4, J. Geophys. Res., 73, 61, 1968.

Sonnerup, B. U. O. and L. J. Cahill, Magnetopause structure and attitude
from Explorer 12 observations, J. Geophys. Res., 72, 171, 1967.

TABLE 1
EXPERIMENTS AND PRINCIPAL INVESTIGATORS

	VOYAGER 1, 2	HELIOS 1, 2	IMP-8
MAGNETOMETER	NESS (GSFC)	MARIANI/NESS (ROME/GSFC)	NESS (GSFC)
PLASMA ANALYZER	BRIDGE (MIT)	ROSENBAUER (MAX-PLANCK/GARCHING)	BRIDGE (MIT)

TABLE 2

SHOCK TIMES

SPACECRAFT	DAY	HR/MIN
VOYAGER 2	JAN. 6	0134
HELIOS 1	JAN. 3	0838
HELIOS 2	JAN. 3	1450
IMP 8	JAN. 3	2041
SSC	JAN. 3	2024

TABLE 3
FILAMENT BOUNDARY NORMALS

DISCONTINUITY	SPACECRAFT	DAY,HR/MIN	λ_n	δ_n
A	V-2	8,1030	235°	-15°
B	V-2	8,1220	230°	0°
A[1]	V-1	8,1440	208°	- 4°

FIGURE CAPTIONS

FIGURE 1   Positions of Voyager 1 and 2, Helios 1 and 2, and IMP (near Earth) in the period January 5-8, 1978. Positions are in inertial heliographic coordinates, (a) being the equatorial plane view and (b) showing the elevation of the spacecraft above (below) the equatorial plane.

FIGURE 2   Voyager 1 observations of a magnetic cloud and associated flow. The data are 4 min averages. The direction of $\underset{\wedge}{B}$ is in solar heliographic coordinates; δ is the latitude ($\delta = 0°$ when $\underset{\wedge}{B}$ is in the equatorial plane and is positive when $\underset{\wedge}{B}$ points northward) and λ is the azimuthal angle ($\lambda = 0$ when $\underset{\wedge}{B}$ points radially away from the sun and increases counter-clockwise when seen from the north). The Voyager 1, 2 temperatures are computed by taking moments of the observed distribution functions.

FIGURE 3   Helios 2 observations of the magnetic cloud and associated flows. Here the direction of $\underset{\wedge}{B}$ is in solar ecliptic coordinates; θ is the latitude ($\theta = 0$ in the ecliptic plane) and ϕ is the azimuthal angle ($\phi = 0$ when $\underset{\wedge}{B}$ points toward the sun).

FIGURE 4   Magnetic field strengths and latitudes measured by V1, V2, H2, and IMP-8.

FIGURE 5   Sketch of the geometry of the cloud. The dots show where the observed boundaries of the cloud would be at 2200 UT on January 6, 1978, assuming that they moved at constant speed. The shape of the cloud is determined by simply connecting the dots, and it is only approximate. This figure shows that the cloud extends at least 30° in the azimuthal direction and $\sim$ 0.5 AU in the radial direction.

FIGURE 6   Results of the minimum variance analysis of hour averages of the magnetic field in the cloud observed by Voyagers 1 and 2. δ_n and λ_n give the normal to the plane of maximum variance in solar heliographic coordinates.

FIGURE 7   Results of the minimum variance analysis of hour averages of the magnetic field observed by IMP-8 and Helios-2. Although the data used were in solar ecliptic coordinates, the directions of the normals are shown in solar heliographic coordinates so that they can be compared with the Voyager results.

FIGURE 8   Sketch of possible magnetic field configuration in the magnetic cloud, based on the minimum variance normals in Figure 6 and Figure 7, and on the shape shown in Figure 5.

FIGURE 9   Density profiles. The V1 and V2 data are 5 min averages; the IMP, H1 annd H2 data are hour averages.

FIGURE 10   Bulk speed profiles. Averages as in Figure 9.

FIGURE 11   Temperature profiles. Averages as in Figure 9.

FIGURE 12   Momentum flux, total pressure (proton plus electron plus magnetic field) and the proton plus electron pressure divided by the magnetic pressure observed by Voyager 1.

FIGURE 13   Momentum flux, total pressure, and pressure ratio observed by Voyager 2 (see Figure 12 caption).

FIGURE 14   Voyager 2 observations of the magnetic cloud and associated flow (parameters as described in caption of Figure 2). Note the unusual filament (AB) on January 8.

FIGURE 15   Filament at high resolution (9.6 sec averages).

FIGURE 16   Momentum flux, total pressure, and pressure ratio (see Figure
               12 caption) across the filament observed by Voyager 2. It is
               an equilibrium structure immersed in a low β plasma.

FIGURE 17   Each line segment is the intersection of a plane with the
               solar equatorial plane (top) or a meridian plane (bottom).
               Three types of planes are shown: 1) current sheets bounding
               the filament (A, A', B) and current sheets in sheath (C, D,
               E); 2) the shock surface, and 3) the plane of maximum
               variance of B in the magnetic cloud, represented by dashed
               line segments arbitrarily placed at the point in the cloud
               where the direction of the magnetic field changed from
               southward (crosses) to northward (dots).

JAN 5-8, 1978

(a)
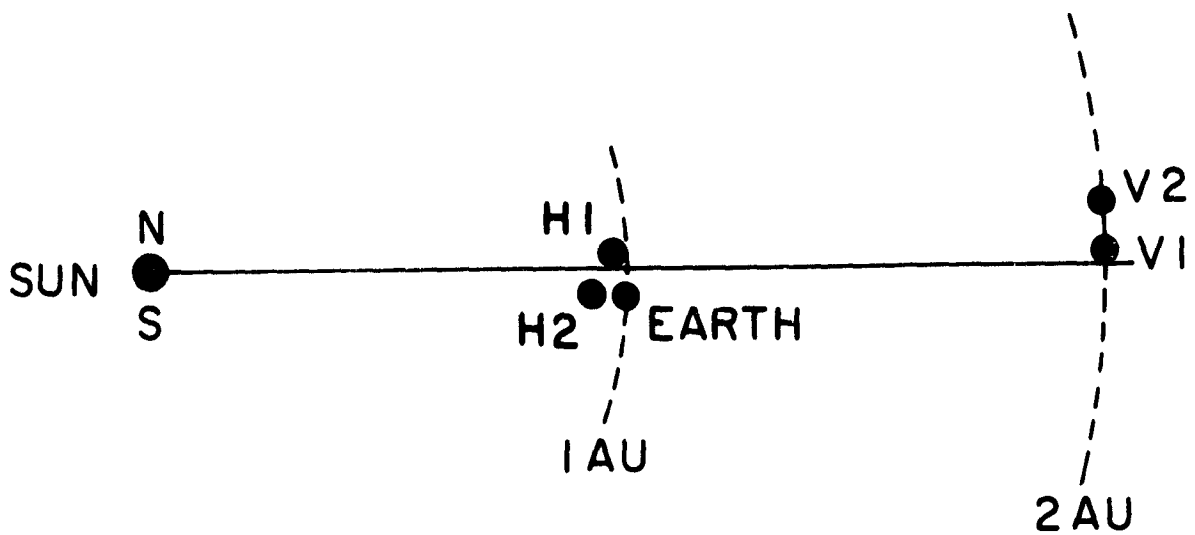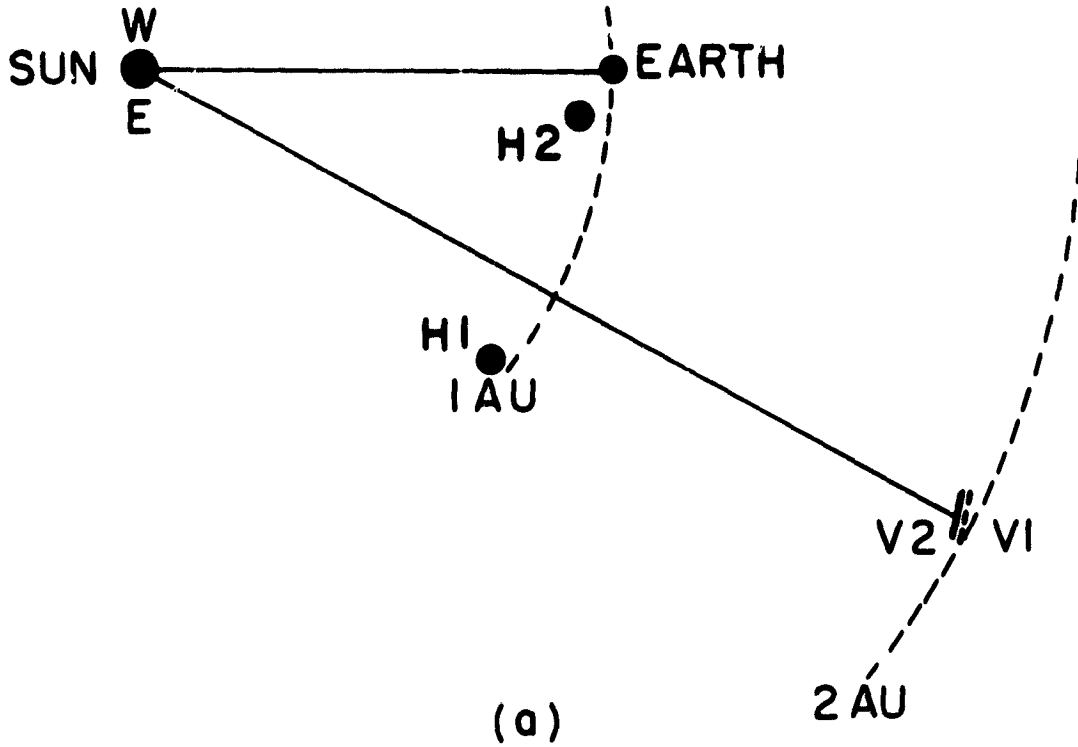
(b)

Figure 1

Figure 2

HELIOS 2

SHOCK

MAGNETIC CLOUD

F (nT)
25

φ
360°
180°
0°

θ
90°
0°
-90°

σ(nT)
12.5
0

T(°K)
10^6
10^5
10^4

n(cm^{-3})
100
10

V
(km/s)
900
600
300

3   4   5   6
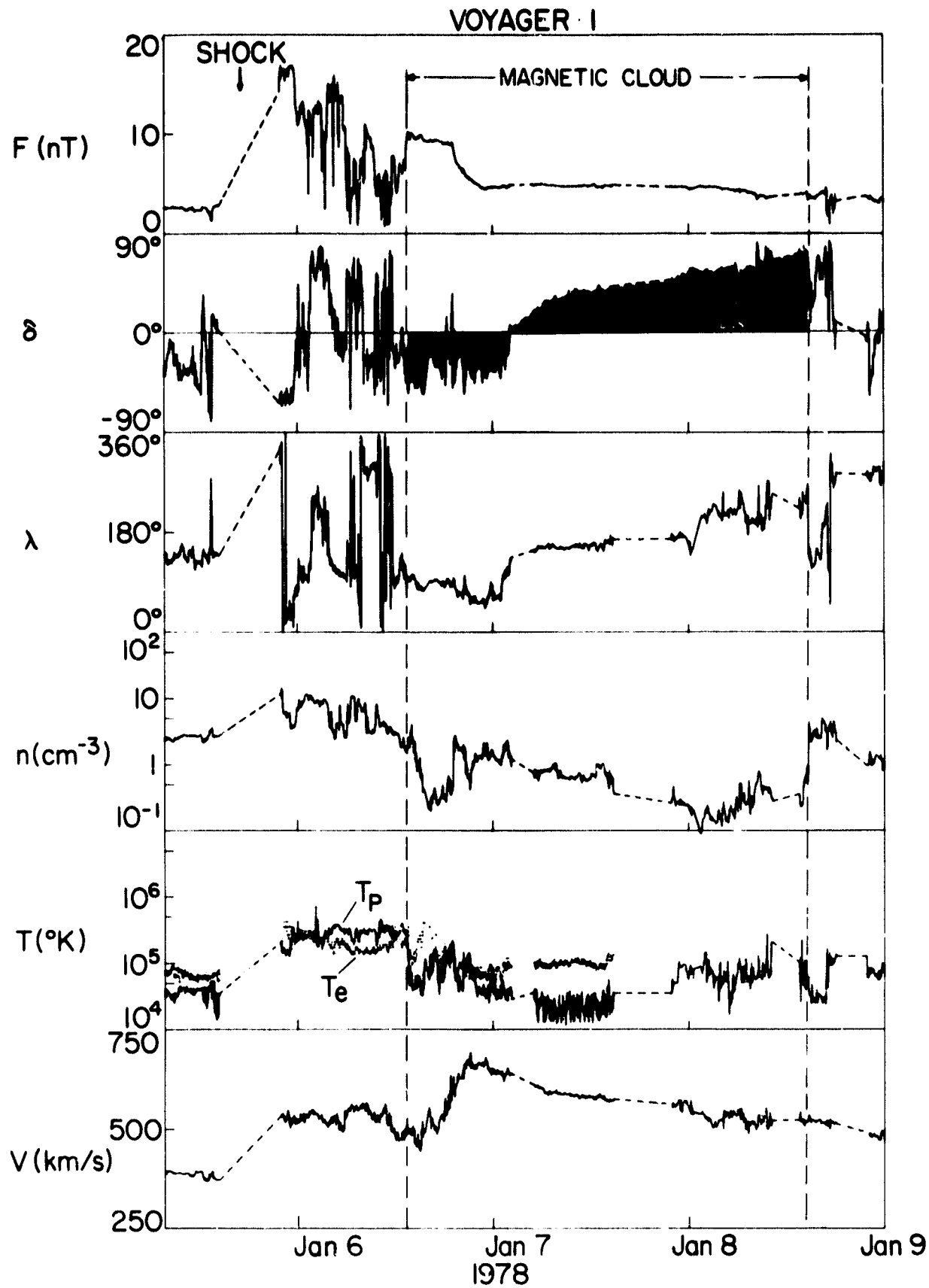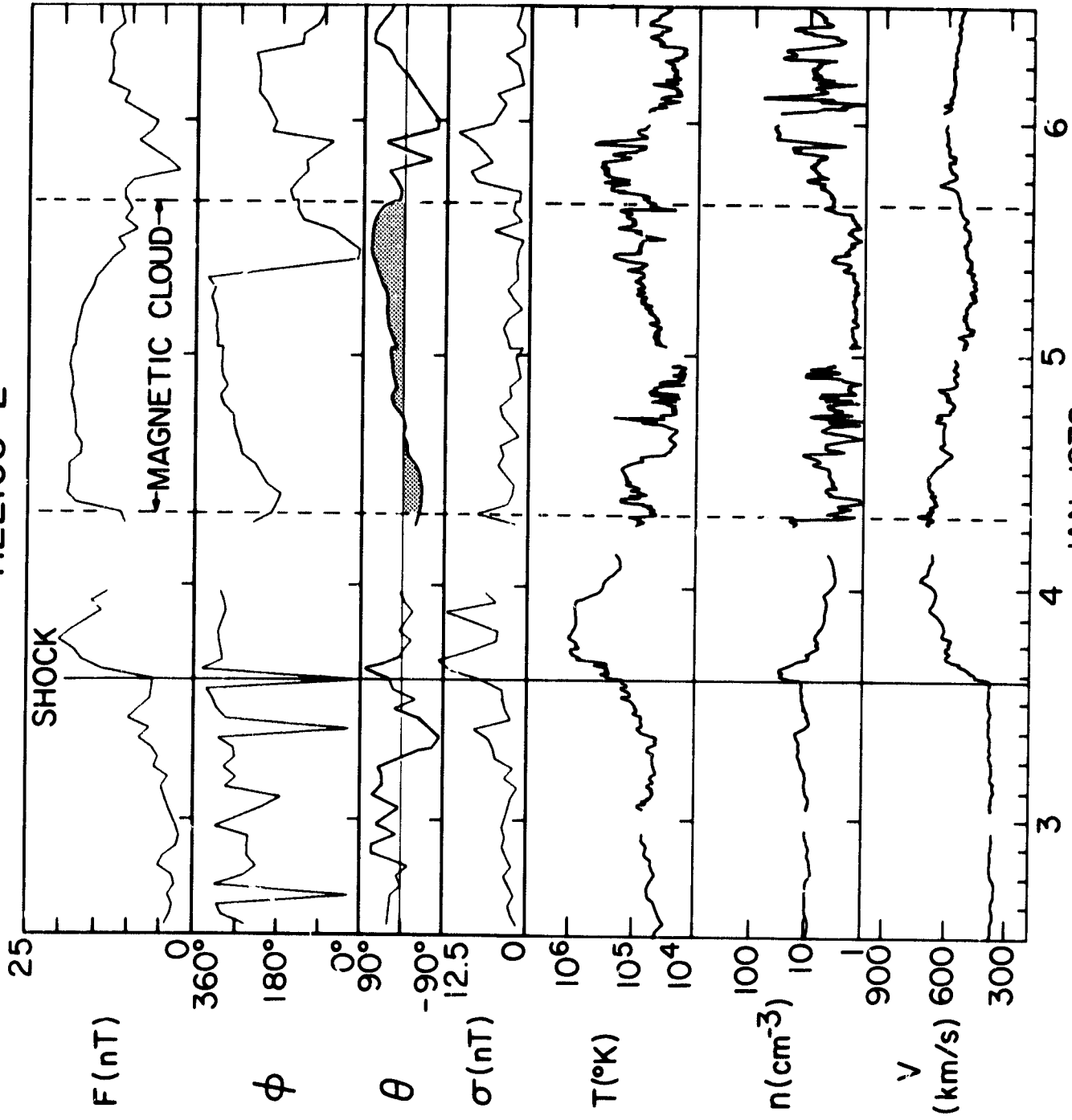
JAN, 1978

Figure 3

1978
Figure 4

SHOCK

SHEATH

MAGNETIC
CLOUD

VOYAGER 1, 2
(2 AU)

IMP 8
(1 AU)

HELIOS 2

HELIOS 1

SUN
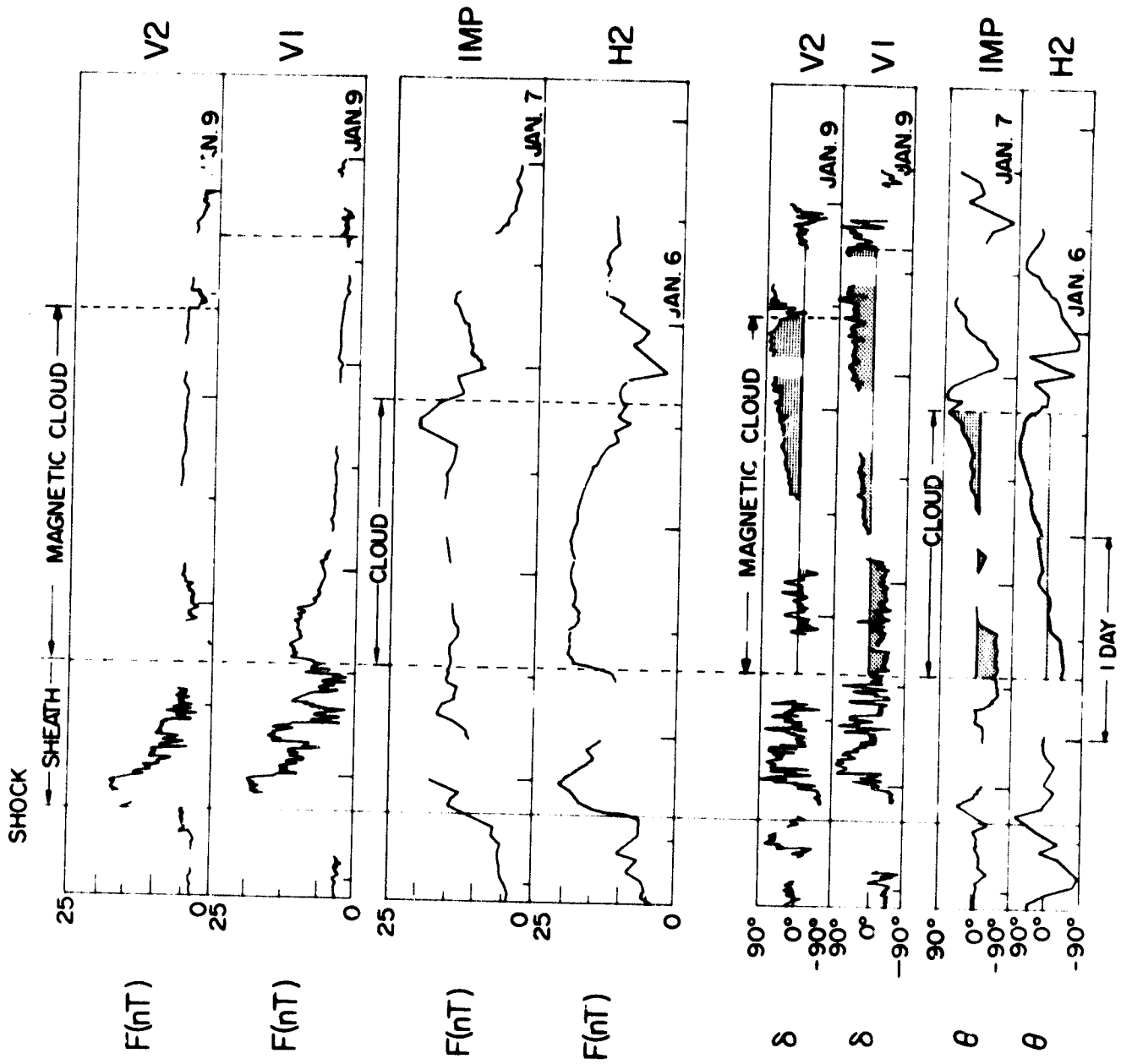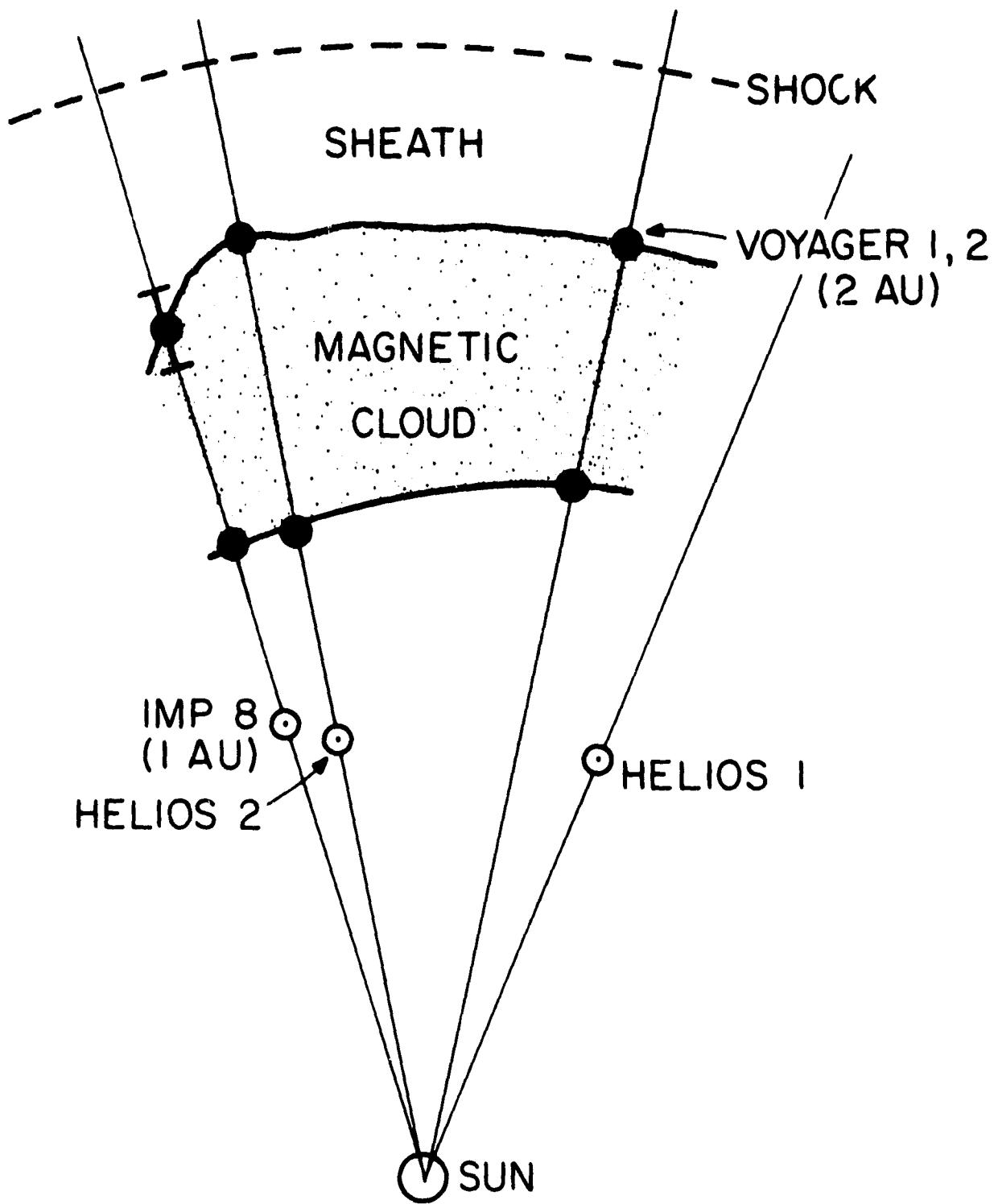
JAN 6, HR 22, 1978
EQUATORIAL PLANE

Figure 5

VOYAGER - 2   VOYAGER - 1

$\lambda_n = 234°$ $\lambda_n = 231°$

$\delta_n = -17°$ $\delta_n = -42°$
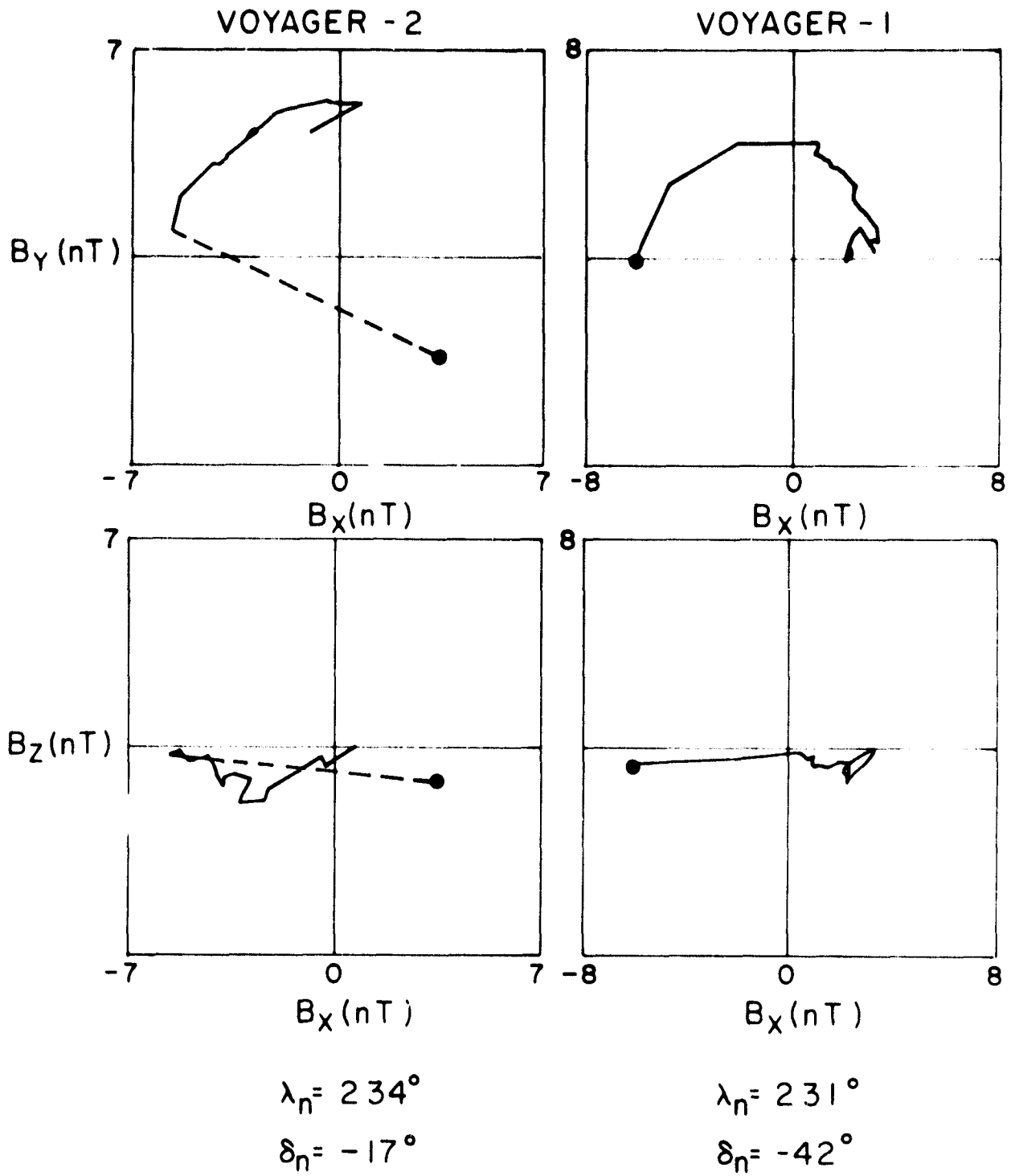
0400, JAN 7 to 1000, JAN 8   2200, JAN 6 to 1400, JAN 8

Figure 6

$\lambda_n = 230°$

$\delta_n = -24°$
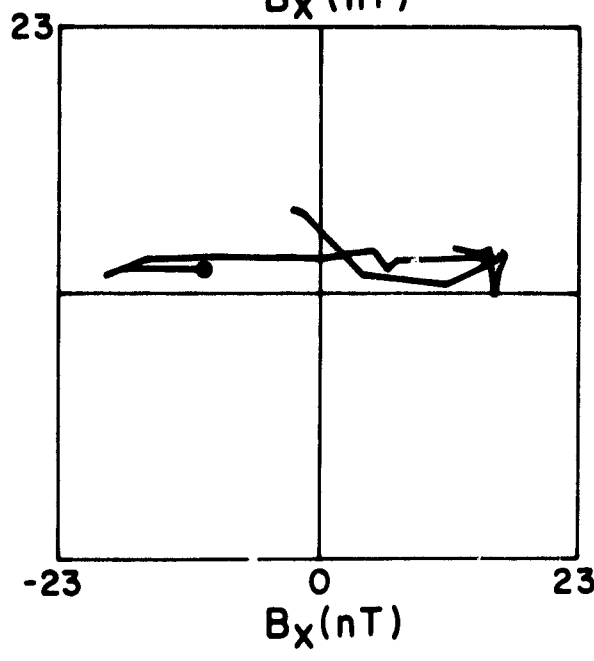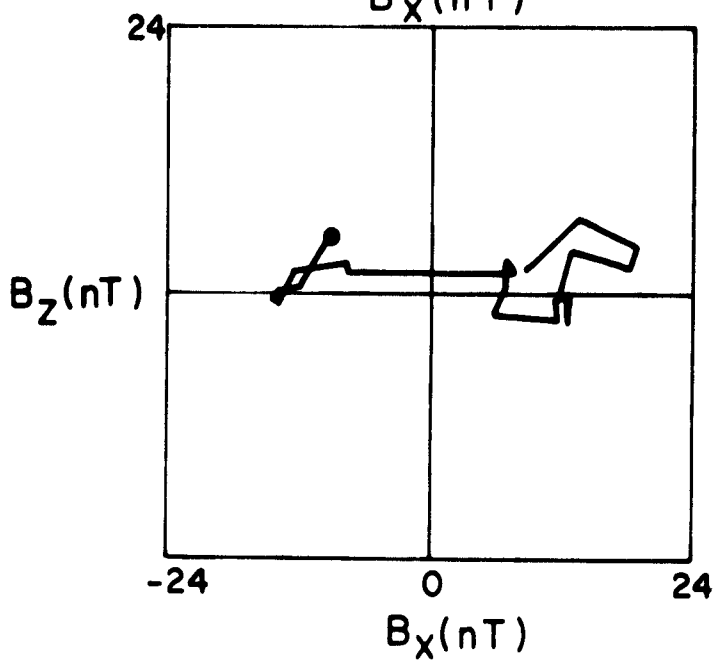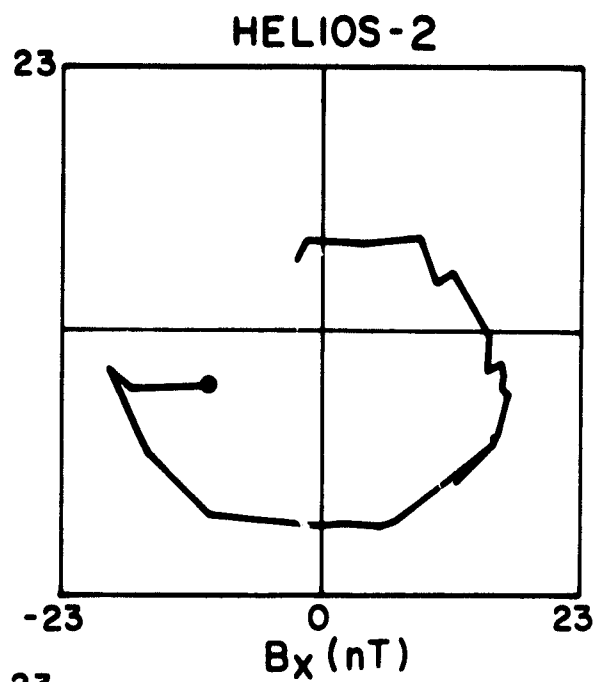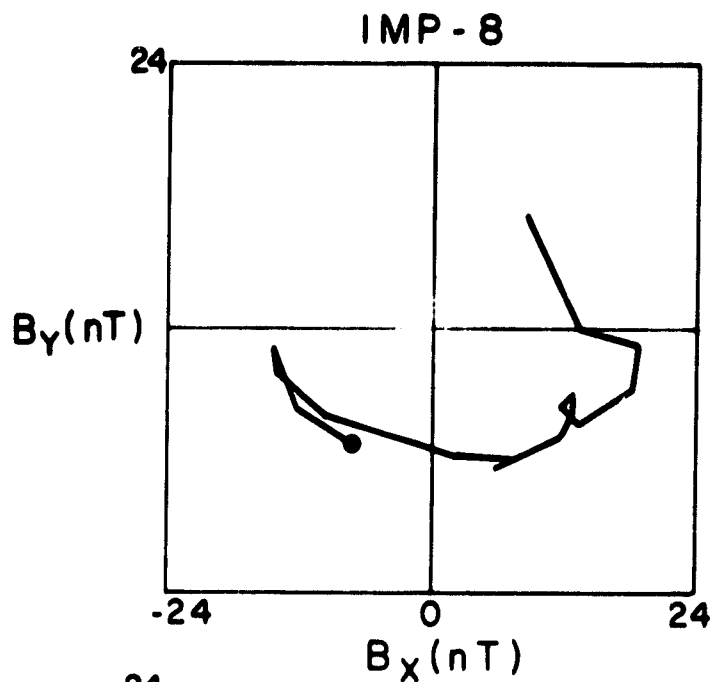
1000, JAN 4 to 2000, JAN 5

$\lambda_n = 203°$

$\delta_n = -46°$

0700, JAN 4 – 1400, JAN 5

Figure 7

MAGNETIC CLOUD

ECLIPTIC PLANE

TO SUN

S/C INTERCEPT

$\hat{R}$

$\hat{n}$

λ_n

δ_n

$\hat{B}$
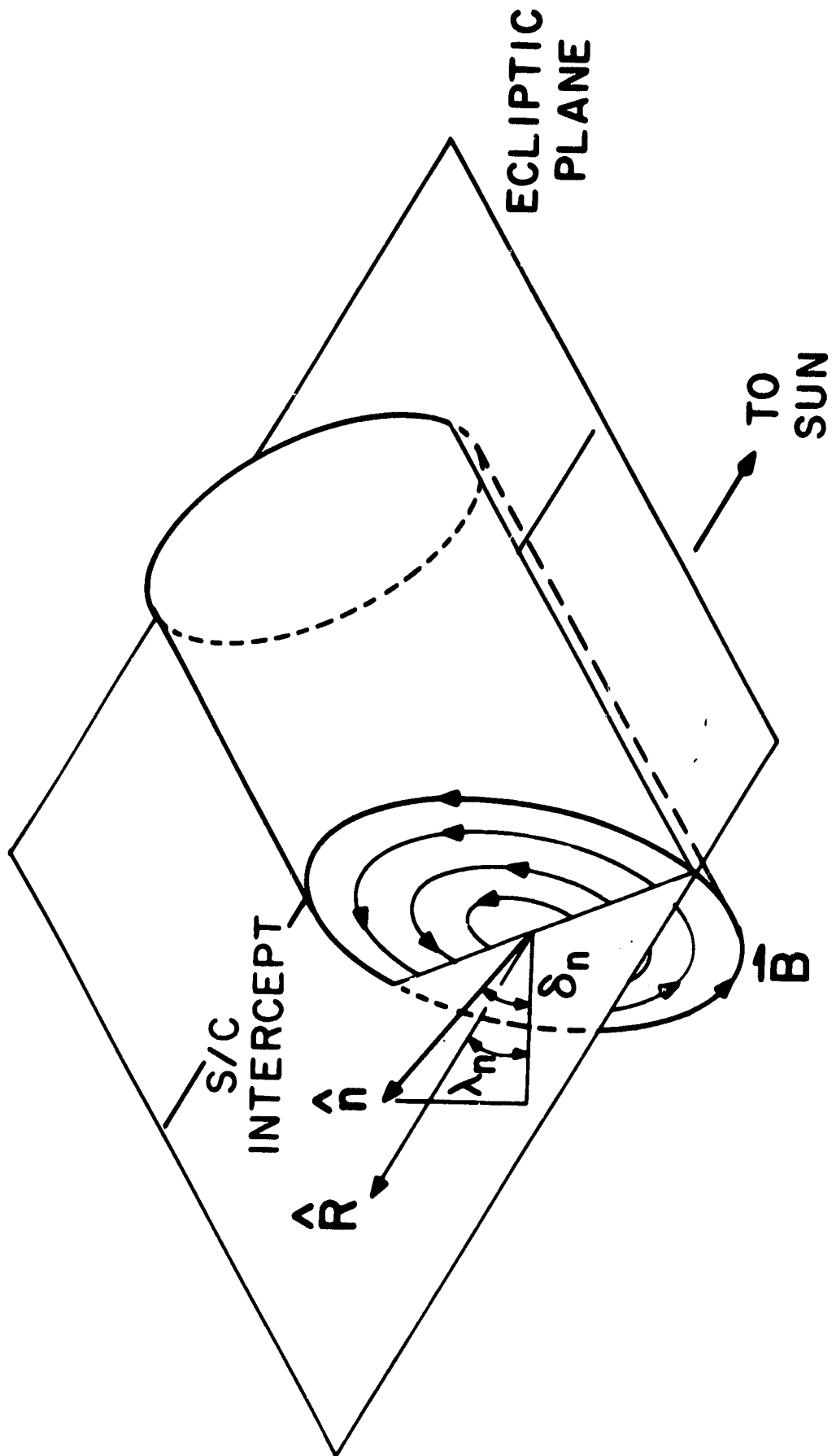
Figure 8
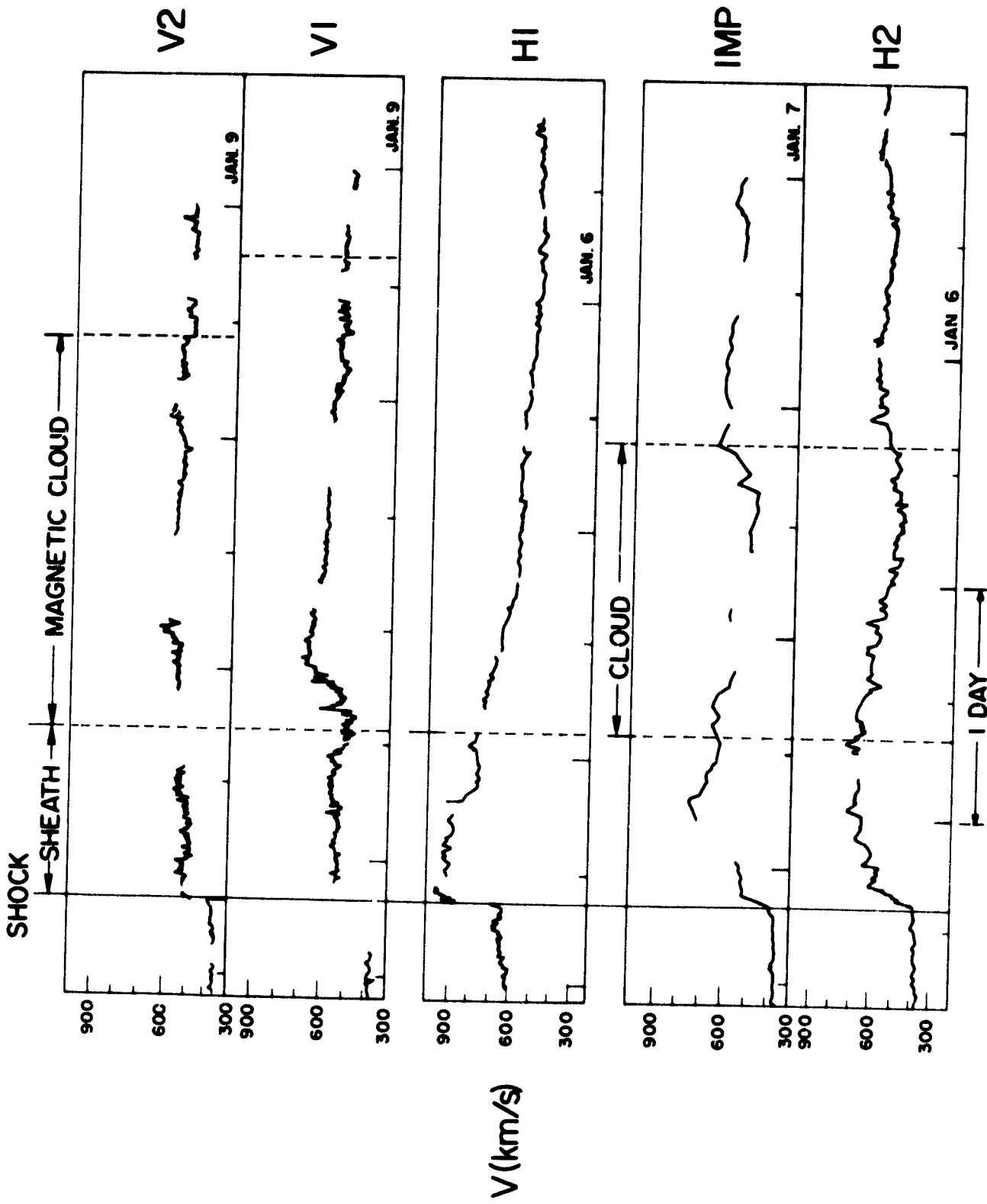
1978

Figure 9

1978

Figure 10

1978

Figure 11

Figure 12

VOYAGER 2

SHOCK

A B

Jan 6 Jan 7 Jan 8 Jan 9
1978

$\rho V^2 (10^{-10} \mathrm{dyn/cm^2})$

$P (10^{-10} \mathrm{dyn/cm^2})$

β_T

Figure 13

VOYAGER 2

F (nT)

δ

λ

n (cm⁻³)

T (°K)

T_P

T_e

V (km/s)

Jan 6   Jan 7   Jan 8   Jan 9

A B
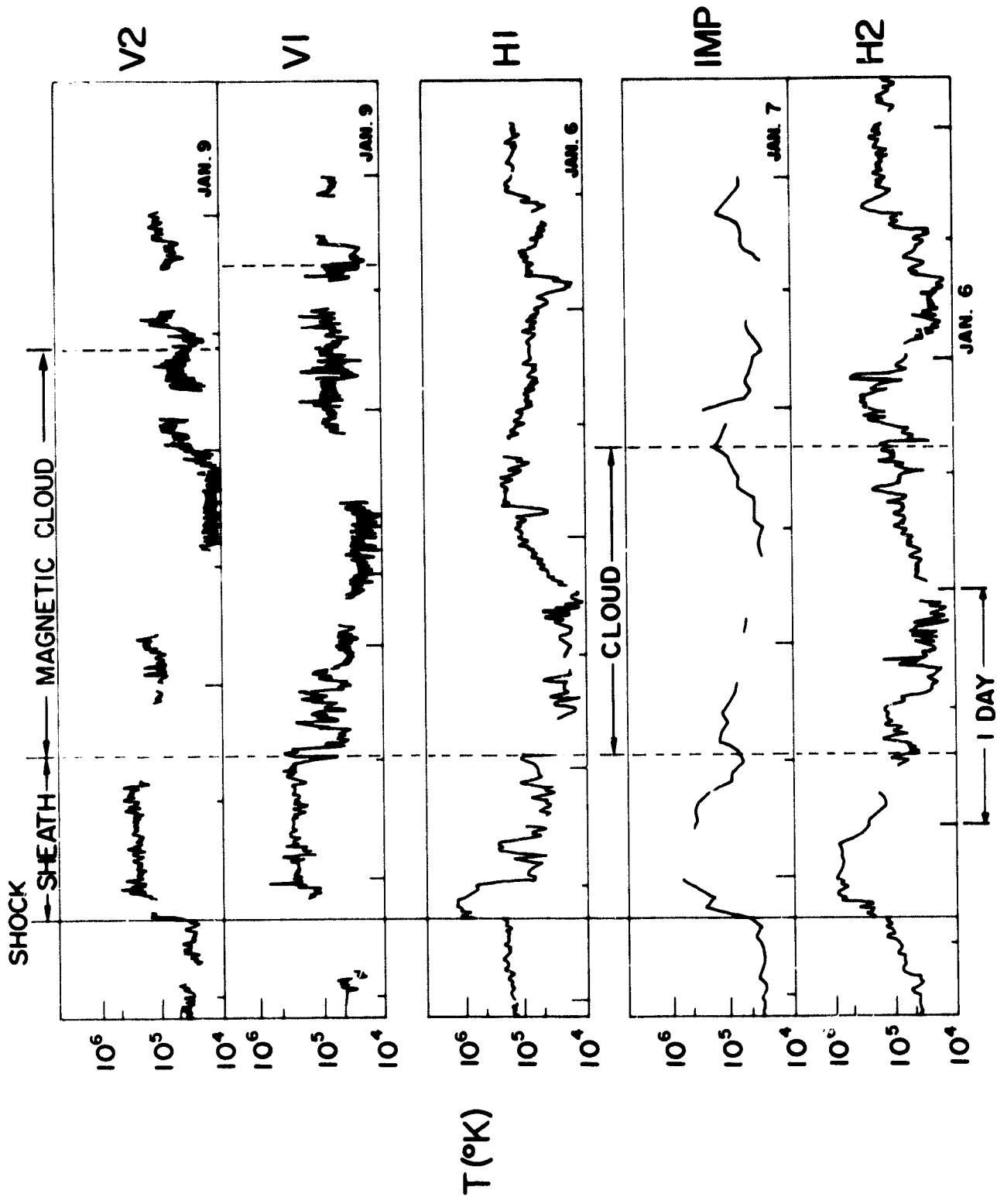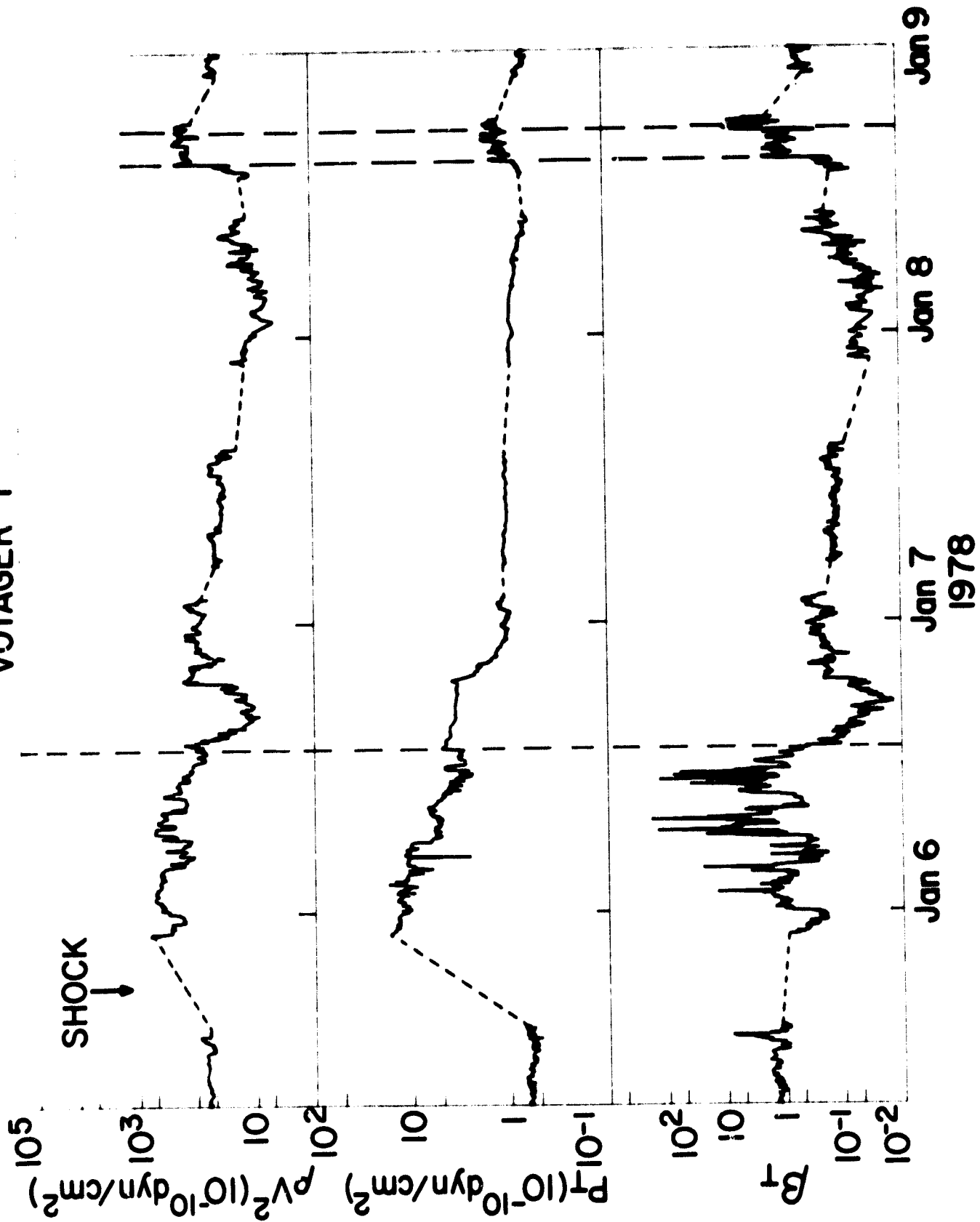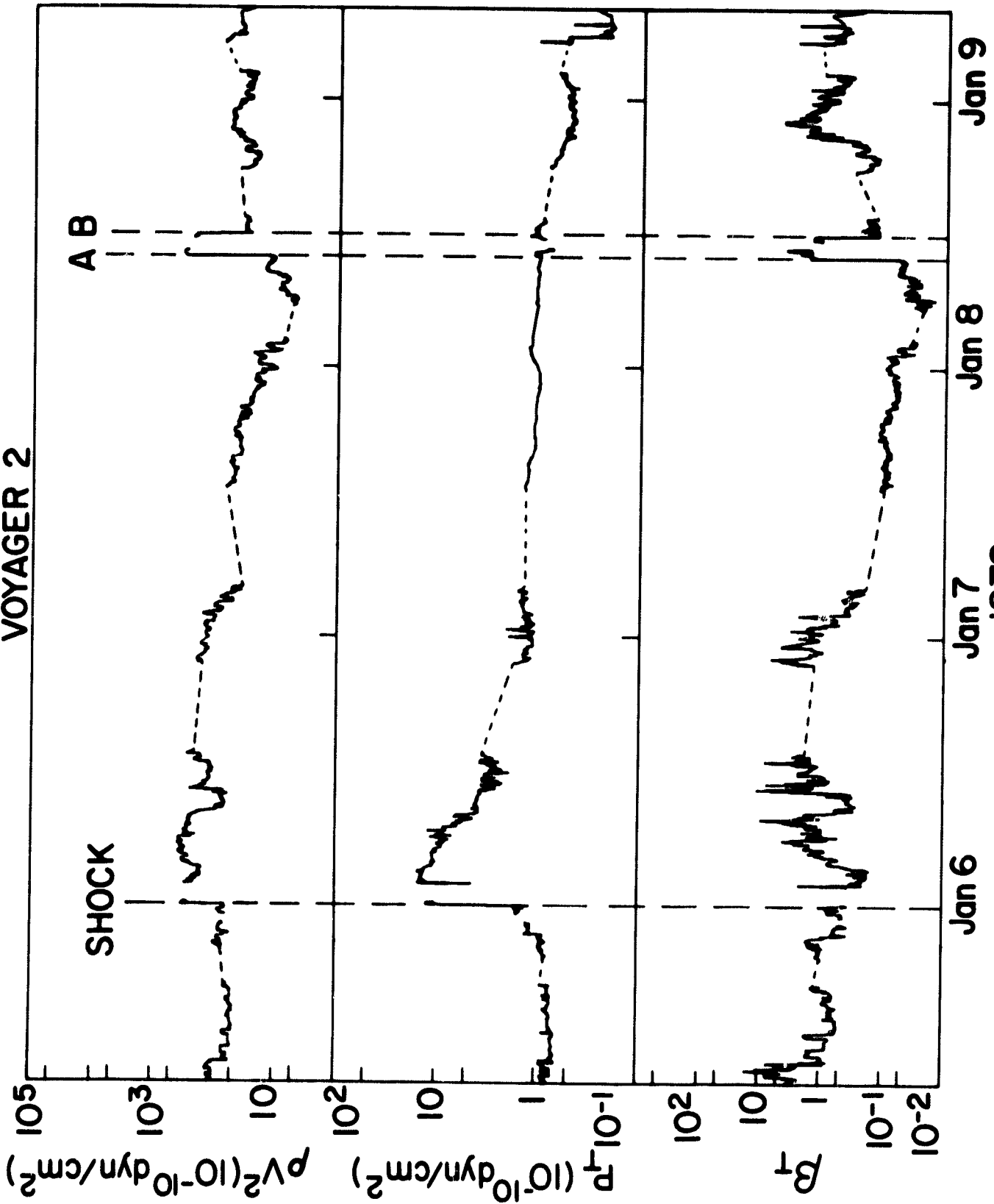
1978
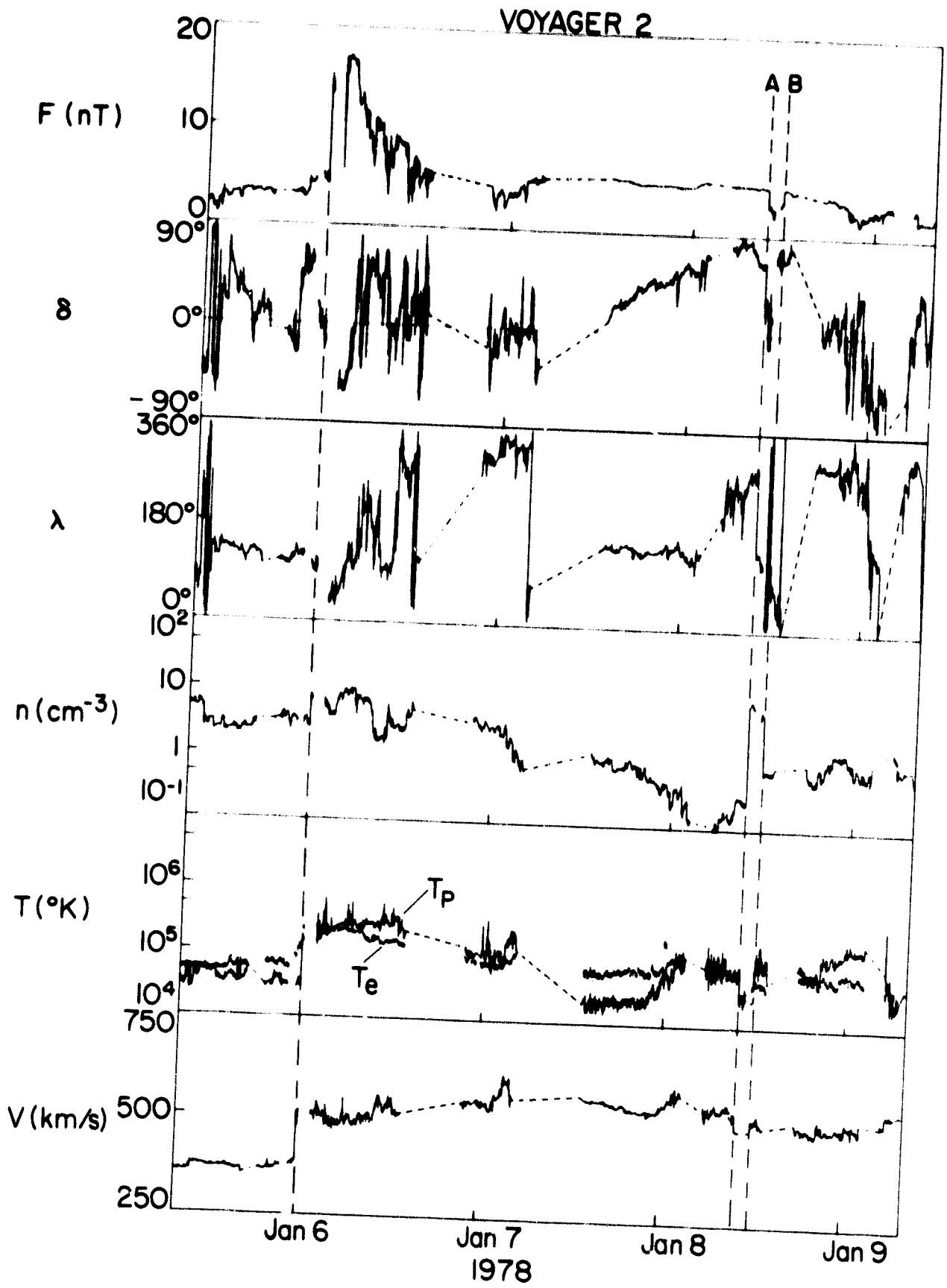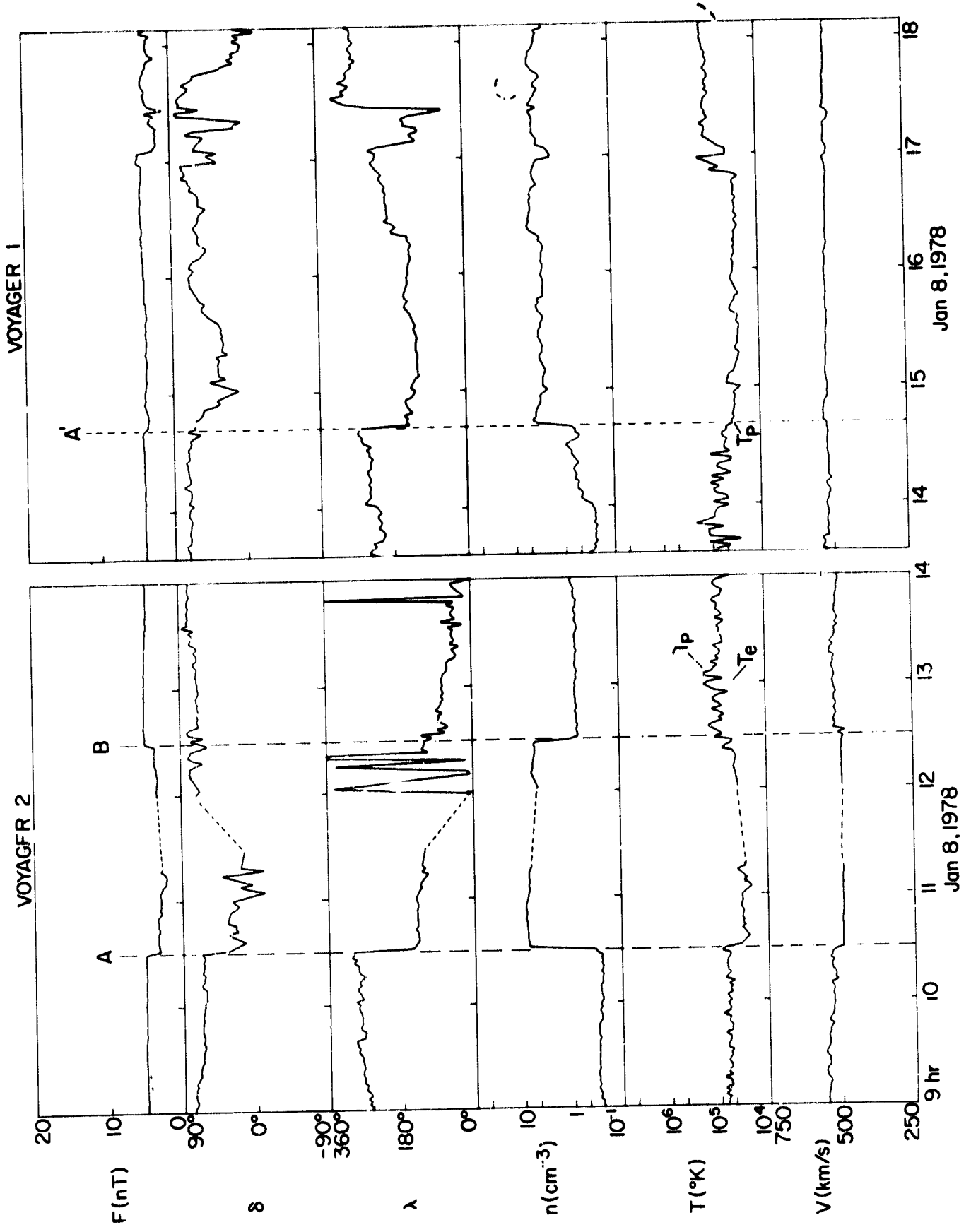
Figure 14

Figure 15

VOYAGER 2

Jan 8, 1972

Figure 16

Figure 17